STOCHASTIC BEHAVIOR OF A QUANTUM PENDULUM UNDER A PERIODIC PERTURBATION

G. Casati

Istituto di Fisica, Via Celoria 16, Milano, Italy

and

B. V. Chirikov and F. M. Izraelev

Institute of Nuclear Physics, 630090 Novosibirsk 90, U.S.S.R.

and

Joseph Ford

School of Physics, Georgia Institute of Technology
Atlanta, Georgia 30332, U.S.A.

ABSTRACT

This paper discusses a numerical technique for computing the quantum solutions of a driven pendulum governed by the Hamiltonian

$$H = (p_\theta^2/2m\ell^2) - [m\ell^2\omega_o^2\cos\theta]\ \delta_p(t/T),$$

where p_θ is angular momentum, θ is angular displacement, m is pendulum mass, ℓ is pendulum length, $\omega_o^2 = g/\ell$ is the small displacement natural frequency, and where $\delta_p(t/T)$ is a periodic delta function of period T. The virtue of this rather singular Hamiltonian system is that both its classical and quantum equations of motion can be reduced to mappings which can be iterated numerically and that, under suitable circumstances, the motion for this system can be wildly chaotic. Indeed, the classical version of this model is known to exhibit certain types of stochastic behavior, and we here seek to verify that similar behavior occurs in the quantum description. In particular, we present evidence that the quantum motion can yield a linear (diffusive-like) growth of average pendulum energy with time and an angular momentum probability distribution which is a time-dependent Gaussian just as does the classical motion. However, there are several surprising distinctions between the classical and quantum motions which are discussed herein.

Since we have not yet developed a completely adequate explanation for all these distinctions, this paper should be regarded as a progress report describing work on a highly interesting and numerically solvable model.

I. INTRODUCTION

Noteworthy recent progress[1-3] has been made in illustrating the truly stochastic behavior which can occur for the strictly deterministic systems of classical mechanics. Indeed, quite simple classical Hamiltonian systems can exhibit precise phase space trajectories so chaotic in their phase space wanderings that slightly imperfect observation cannot distinguish this deterministic motion from completely stochastic motion. Even though some of these model systems have only a few degrees of freedom, they nonetheless illustrate a generic type of wild classical mechanical trajectory behavior which is of great significance in the study of dynamical stability and of statistical mechanics; moreover, the nature of such wild behavior is now being studied for more general systems of widespread physical interest. Thus, even at this early stage, it becomes highly desirable to establish the effect introduced by quantum mechanics on this classical mechanical stochastic behavior. For even more than in classical mechanics, most of the exact work in quantum mechanics has been devoted to integrable (solvable) systems, with the remaining more difficult problems being left either to generally divergent perturbation theory or to quantum statistical mechanics whose foundations are less well understood than those of classical statistical mechanics. As a consequence, there is not only a dearth of quantum models exhibiting stochastic behavior, there is also some ambiguity even concerning the criteria for and the definition of quantum stochastic behavior.

Thus a number of recent papers have appeared, using a variety of techniques, which seek to develop viable criteria for and a definition of quantum stochastic behavior. To establish their criterion, Pukhov, et. al.,[4] generalize the notion of local instability (exponential separation) of initially close orbits valid for classical stochastic systems. In particular, they investigate the time growth of the change in the wave function $\delta\psi$ due to a small external perturbation added to the original Hamiltonian, and they establish criteria sufficient to insure an exponential growth in $\delta\psi$. Along somewhat related lines, Percival and Pomphrey[5] treat quantum mechanically a Hamiltonian system known to exhibit a classical transition from near-integrable to

stochastic behavior. They show that the quantum energy levels for this Hamiltonian become highly sensitive to very small added external perturbations only above the classical stochastic threshold, and they argue that their study thus reveals a transition to quantum stochastic behavior. Both of these studies investigate quantum stochasticity as revealed through small but explicit outside perturbations.

The works of Nordholm and Rice[6,7] and of Shuryak[8] are more directly concerned with the case of isolated Hamiltonian systems for which the Hamiltonian splits naturally into dominant terms describing independent degrees of freedom which are coupled by small nonlinear interaction terms. Nordholm and Rice[6] also present a brief but clear review of the older literature on quantum ergodic theory for isolated systems, pointing out that this problem is still very much an open one. Both Nordholm and Rice as well as Shuryak regard their isolated quantum systems as behaving stochastically when the unperturbed eigenstates of the dominant, independent modes are strongly coupled by the weak interaction in the sense that the expansion of the exact quantum state is a sum of many unperturbed, independent mode states. The approach of Nordholm and Rice is, in principle, exact but in practice is forced to rely heavily on numerical (computer) computations whereas the work of Shuryak is strictly analytic but only approximate since it is based on a generalization of the order of magnitude resonance-overlap estimates of Chirikov.[3] For further details on work in this area, the reader is referred to the papers listed as Reference 9. Additional discussions of quantum stochasticity appear, of course, in several of the companion papers in this volume.

But strangely enough, to our knowledge, no quantum investigation has previously been made for the simplest possible Hamiltonian system known to exhibit chaotic trajectories, namely a periodically driven (i.e., time-dependent) one degree of freedom Hamiltonian system. Perhaps this is because such driven systems are, in general, no easier to solve than the conservative two degree of freedom systems whose quantum behavior has been previously studied. However, there is one notable exception to this general rule, and it is this exception which we seek to exploit in this paper. In particular, both the classical and quantum equations of motion for pendulum Hamiltonians of the type

$$H = (p_\theta/2m\ell^2) + V(\theta)\ \delta_p(t/T)\ , \qquad (1)$$

where θ is angular displacement, p_θ is angular momentum, m is pendulum mass, ℓ is pendulum length, $V(\theta)$ is angular potential energy, and

$\delta_p(t/T)$ is a periodic delta function of period T, can be reduced to mappings and solved numerically as we shall show. Indeed, the classical motion for Hamiltonian (1) using $V(\theta) = -mg\ell\cos\theta = -m\ell^2\omega_o^2\cos\theta$ has already been extensively investigated,[3] and it is for this reason that we chose to begin our quantum studies using this particular model.

In Section II, we derive the classical mapping equations for our model and discuss the nature of its solutions. In Section III, we derive and discuss the quantum mapping equations. Section IV presents our numerical results for the quantum problem and these results are then discussed in Section V. Brief concluding remarks appear in Section VI. This paper represents a progress report describing calculations on an exceptional type of driven quantum system which can be solved, at least numerically. It is our hope that future studies on this or related model systems may lead to a broader understanding of quantum chaotic behavior.

II. DISCUSSION OF THE CLASSICAL MODEL

The specific Hamiltonian we choose to study is given by

$$H = (p_\theta/2m\ell^2) - [m\ell^2\omega_o^2\cos\theta]\ \delta_p(t/T)\ , \tag{2}$$

which is merely Hamiltonian (1) specialized to $V(\theta) = -mg\ell\cos\theta = -m\ell^2\omega_o^2\cos\theta$, where obviously $\omega_o^2 = g/\ell$. Here the periodic delta function, which may be expressed as

$$\delta_p(t/T) = \sum_{j=-\infty}^{\infty} \delta[j-(t/T)] = 1+2\sum_{n=1}^{\infty} \cos(2n\pi t/T)\ , \tag{3}$$

"turns on" the gravitational potential for a brief instant during each period T. The classical equations of motion for Hamiltonian (2) are

$$\dot{p}_\theta = -(m\ell^2\omega_o^2\sin\theta)\ \delta_p(t/T) \tag{4a}$$

$$\dot{\theta} = p_\theta/m\ell^2 \tag{4b}$$

where the dot notation indicates time derivative. Letting θ_n and $(p_\theta)_n$ be the values of θ and p_θ just before the nth delta function "kick", we may integrate Eq. (4a,b) to obtain the mapping equations

$$(p_\theta)_{n+1} = (p_\theta)_n - m\ell^2\omega_o^2 T\sin\theta_n\ , \tag{5a}$$

$$\theta_{n+1} = \theta_n + (p_\theta)_{n+1} T/m\ell^2 \quad . \tag{5b}$$

As an aside, let us observe that, when T tends to zero allowing us to replace T by dt, Eq. (5a,b) becomes

$$dp_\theta = -(m\ell^2\omega_o^2 \sin\theta)\, dt \tag{6a}$$

$$d\theta = (p_\theta/m\ell^2)\, dt \quad , \tag{6b}$$

which are precisely the equations of motion for the conservative, gravitational pendulum Hamiltonian

$$H = (p_\theta^2/2m\ell^2) - mg\ell\cos\theta \tag{7}$$

recalling that $\omega_o^2 = g/\ell$. Thus as the time T between delta function "kicks" tends to zero, the gravitational potential is "turned on" continuously and the motion generated by Hamiltonian (2) becomes identical with that generated by the integrable[1] Hamiltonian (7). As T increases away from zero, the orbits of Hamiltonian (2) increasingly deviate from those of the integrable pendulum, eventually exhibiting chaotic or stochastic behavior. Consequently, one may adopt either of two viewpoints regarding Hamiltonian (2). As written above in Eq. (2), it obviously describes a free rotator perturbed by delta function "kicks". The remarks of this paragraph show that Hamiltonian (2) may also be regarded as describing a gravitational pendulum perturbed by a periodic driving force. This latter viewpoint becomes clearer if we rewrite Hamiltonian (2), using Eq. (3), as

$$H = [(p_\theta/2m\ell^2) - mg\ell\cos\theta] - 2mg\ell\cos\theta \sum_{n=1}^{\infty} \cos(2n\pi t/T) \tag{8}$$

In particular, it is the viewpoint represented by Hamiltonian (8) that led to the title of this paper.

Returning to Eq. (5a,b), let us now define the dimensionless angular momentum P_n via the equation $P_n = (p_\theta)_n T/m\ell^2$, and then let us write Eq. (5a,b) in the so-called standard form[3]

$$P_{n+1} = P_n - K\sin\theta_n \tag{9a}$$

$$\theta_{n+1} = \theta_n + P_{n+1} \ , \tag{9b}$$

where $K = (\omega_o T)^2$ is the only remaining mapping parameter. As mentioned earlier when K tends to zero, this mapping becomes precisely integrable with all orbits lying on (or forming) simple invariant curves of the mapping. When K is small, the KAM theorem[2] insures that the mapping is near-integrable, meaning here that most mapping orbits continue to lie on simple invariant curves. Numerical computations[3,10] show that at least some of these simple invariant curves persist as K approaches unity. Moreover, for the K region $0<K<1$, the momentum variation is bounded with $|\Delta P| \lesssim K^{1/2}$. As K reaches and exceeds unity, all the previously existing simple invariant curves completely disappear and most mapping orbits become chaotic point sets. For $K>>1$, numerical evidence shows that the P-motion is characterized by a simple, random walk diffusion equation having the form

$$\overline{P^2} \approx (K^2/2)t \ , \tag{10}$$

where $\overline{P^2}$ is the average of the squared angular momentum at integer time $t = n$ measured in units of the period T and where initially P is taken to be zero. The average here is over many orbits having distinct θ_o initial conditions or over many sections of the same orbit (normalizing P to zero at the beginning of each segment). In order to indicate the source of Eq. (10), let us note that from Eq. (9a) we may obtain

$$(P_n - P_o)^2 = K^2 \sum_{j,k=o}^{(n-1)} (\sin\theta_j \sin\theta_k) \ . \tag{11}$$

Averaging Eq. (11) over θ_j and θ_k, taking both to be uniformly distributed random variables, yields Eq. (10); this procedure is validated by numerical iteration of chaotic orbits. But in addition to Eq. (10), the empirically observed angular momentum distribution itself has the time-dependent Gaussian form

$$f(P) = [K(\pi t)^{1/2}]^{-1} \exp[-P^2/K^2 t] \ , \tag{12}$$

as would be expected from the central limit theorem provided we regard P_n in the equation $P_n = P_o - K \sum_{j=o}^{(n-1)} \sin\theta_j$ as being a sum of random variables. It is precisely this stochastic momentum (or energy) diffusion we shall seek to empirically observe in the quantum description of this model to which we now turn.

III. DISCUSSION OF THE QUANTUM MODEL

We now seek to solve Schrodinger's equation

$$H\psi(\theta,t) = i\hbar\,\partial\psi(\theta,t)/\partial t \tag{13}$$

for the system governed by Hamiltonian (2). In this section, we regard the system as a free rotator perturbed by delta function "kicks" and we expand the wave function $\psi(\theta,t)$ in terms of the free rotator eigenfunctions $(2\pi)^{-1}e^{in\theta}$. In particular, we write

$$\psi(\theta,t) = (2\pi)^{-1}\sum_{n=-\infty}^{\infty} A_n(t)e^{in\theta} \quad . \tag{14}$$

Over any period T between delta function "kicks", the $A_n(t)$ evolve according to

$$A_n(t+T) = A_n(t)e^{-E_nT/\hbar} = A_n(t)e^{-in^2\tau/2} \quad , \tag{15}$$

where

$$E_n = n^2\hbar^2/2m\ell^2 \tag{16}$$

are the free rotator energy eigenvalues and where

$$\tau = \hbar\, T/m\ell^2 \quad . \tag{17}$$

During the infinitesimal time interval of a "kick", we may write Eq. (13) as

$$i\hbar\partial\psi/\partial t = -m\ell^2\omega_o^2\cos\theta\,\delta_p(t/T)\psi \quad . \tag{18}$$

Integrating Eq. (18) over the infinitesimal interval (t+T) to $(t+T^+)$, we find

$$\psi(\theta,t+T^+) = \psi(\theta,t+T)\; e^{ik\cos\theta} \quad , \tag{19}$$

where

$$k = (m\ell^2\omega_o^2T)/\hbar) \quad . \tag{20}$$

Now expanding both sides of Eq. (19) in free rotator eigenfunctions yields

$$\sum_{n=-\infty}^{\infty} A_n(t+T^+)\ e^{in\theta} = \sum_{r,s=-\infty}^{\infty} A_r(t+T)b_s(k)\ e^{i(r+s)\theta}, \tag{21}$$

where we have used the expansion

$$e^{ikcos\theta} = \sum_{s=-\infty}^{\infty} b_s(k)\ e^{is\theta} \tag{22}$$

with $b_s(k) = i^s J_s(k) = b_{-s}(k)$ and with $J_s(k)$ being the ordinary Bessel function of the first kind. Because of the orthogonality of the $e^{in\theta}$, we may use Eq. (21) to establish that

$$A_n(t+T^+) = \sum_{r=-\infty}^{\infty} A_r(t+T)b_{n-r}(k) \quad . \tag{23}$$

Finally using Eq. (15), we obtain the quantum mapping

$$A_n(t+T^+) = \sum_{r=-\infty}^{\infty} A_r(t)b_{n-r}(k)\ e^{-ir^2\tau/2} \tag{24}$$

giving the A_n at time $(t+T^+)$ in terms of the A_n at time t. Using Eq. (24) and Eq. (14), we could obtain $\psi(\theta,t+T^+)$ in terms of $\psi(\theta,t)$, but in the calculations of interest here, the A_n momentum-representation is more useful. Before turning to these calculations however, let us briefly discuss the quantum mapping of Eq. (24).

First, let us note that the mapping of Eq. (24) can actually be numerically iterated to obtain the time development of a quantum solution provided only one or a few of the initial $A_n(0)$ are non-zero. Even though the sum on r is infinite, the $b_s(k) = i^s J_s(k)$ coefficients become negligible[11] outside the range $s \lesssim 2k$. Thus for reasonable sized k-values starting from only one (or a few) initially non-zero $A_n(0)$, we may iterate through many periods T before the increasing number of non-zero $A_n(t)$ exceeds the practical limitations of a large computer. Moreover, accuracy can be monitored via the normalization condition $\Sigma\ |A_n|^2 = 1$. Next, let us observe that the classical mapping depends on the single parameter $K = (\omega_o T)^2$. Thus one might, at first glance, expect the quantum mapping to depend only on the product $(k\tau)$ since $K = (k\tau)$ as one may immediately verify from Eq. (17,20). Indeed Ehrenfest's theorem makes it reasonable to suppose that the product $K = k\tau$ is particularly significant since it would control the time

evolution of the center of a wave packet; however, the additional quantum spreading of the packet might not depend on this product alone. Not only does the numerical evidence presented later indicate that the quantum mapping does indeed depend separately on k and τ, but examination of Eq. (24) itself shows that this must be the case. First, independent of the value of k, Eq. (24) is invariant to the replacement of τ by $(\tau+4\pi)$; thus contrary to the classical case, the quantum motion places an upper bound on τ (or T), since in Eq. (24) there is no loss of generality in restricting τ to the interval $0 \leq \tau \leq 4\pi$. This quantum anomaly arises because the wave function for the unperturbed free rotator is periodic in τ independent of initial conditions. Also in Eq. (24) when $k<1$, only one or a very few $b_s(k)$ coefficients will be appreciably different from zero. For both these reasons, one would expect the classical and quantum motion to differ greatly when K is large due to a small k and a large τ. This is only one of a variety of perhaps interrelated classical-quantum distinctions. Finally since from Eq. (19) it is clear that k is the parameter which controls the amount of energy absorbed by the rotator due to the driving delta function "kicks", it may be worthwhile to use Eq. (20) and write Hamiltonian (2) as

$$H = (p_\theta/2m\ell^2) - (\hbar k T^{-1}\cos\theta)\ \delta_p(t/T) \quad , \tag{25}$$

thus revealing k as an explicit coupling parameter.

IV. NUMERICAL RESULTS FOR THE QUANTUM MODEL

For the quantum model discussed in Sec. III, we have numerically iterated Eq. (24) to obtain the time evolved $\{A_n(t)\}$ starting from various initial $\{A_n(0)\}$ sets. For each computer run, starting with a definite $\{A_n(0)\}$ set, we calculated at each iteration the probability distribution

$$\rho(n) = |A_n|^2 \quad , \tag{26}$$

the average energy (in units of $\hbar^2/m\ell^2$)

$$\langle E \rangle = \sum_n (n^2/2)\ \rho(n) \quad , \tag{27}$$

and the average angular momentum (in units of $\hbar$)

$$\langle p_\theta \rangle = \sum_n n\rho(n) \quad . \tag{28}$$

In all runs after fixing k and τ, we chose only one $A_n(0)$ or a few ($\sim$10) adjacent $A_n(0)$ to be non-zero. Surprisingly, the computed final state $\rho(n)$ appeared to be independent of the precise initial state, a point to which we return later. Typical results for four runs are discussed below. Each of these four runs was started with only the ground state free rotator $A_0(0)$ being non-zero.

In order to investigate the extent to which the numerically computed quantum distribution $\rho(n)$ of Eq. (26) mimics the classical stochastic distribution of Eq. (12), let us write Eq. (12) in terms of the quantum variables. Using the definitions of τ, P, and K and the fact that $p_\theta = n\hbar$, we may write the quantum version of Eq. (12) as

$$f(n) = [k(\pi t)^{1/2}]^{-1} \exp(-n^2/k^2 t) \tag{29}$$

where t is integer time measured in multiples of the "kick" period T. Note in Eq. (29) the dependence on k rather than K (=kτ). If the quantum system indeed mimics the classical motion for $K = k\tau >> 1$, then we would expect the $\rho(n)$ of Eq. (26) to equal the f(n) of Eq. (29), since loosely speaking the quantum solution is an "automatic" average over many classical orbits. For ease of graphical comparison, let us introduce the normalized variables $X = n^2/k^2 t$, $f_N(n) = k(\pi t)^{1/2} f(n)$, and $\rho_N(n) = k(\pi t)^{1/2}\rho(n)$; in these variables we need only determine the validity of the simple equation

$$\rho_N(n) = f_N(n) = e^{-X} \quad . \tag{30}$$

For k = 40 and τ = 1/8, we plot the numerically determined ($\ell n \rho_N$) versus X at t = 25 in Fig. 1. The straight line $\ell n(e^{-X}) = \ell n f_N(n)$ is graphed for comparison. One notes here that the comparison is rather good indicating that the quantum motion indeed appears to be stochastic here. It must be noted in Fig. 1 that each plotted point for $\ell n \rho_N(n)$ actually represents an average value of this quantity taken over ten adjacent energy levels; this averaging reduces but does not eliminate fluctuations. In Fig. 2 we present a graph of $\rho_N(n)$ and $f_N(n)$ for the parameter values k = 10 and τ = 1/2. In Fig. 2, contrary to Fig. 1, one notes that the quantum system is not behaving stochastically despite the fact that the classical value of K is five for

both cases and, classically, stochasticity would be expected for both. This is yet another of the several

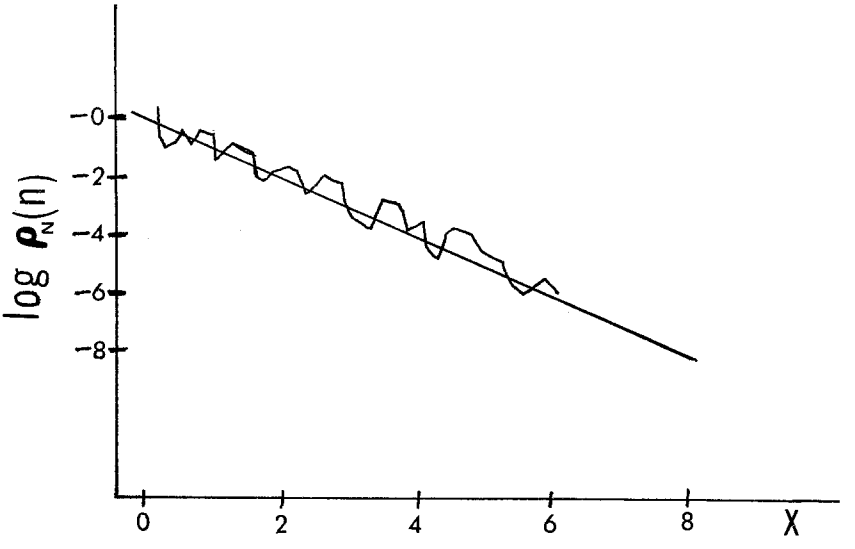

Fig. 1. A plot of the logarithm of the quantum probability distribution $\rho(n)$ versus the normalized variable $X = n^2/k^2t$ at time $t = 25$ for $k = 40$ and $\tau = 1/8$ ($K = 5$). The straight line is a plot of $\ell n(e^{-X})$. Were the quantum motion stochastic, these two curves should be identical; the fact that they are quite close indicates a great similarity between the classical and quantum motion for this case.

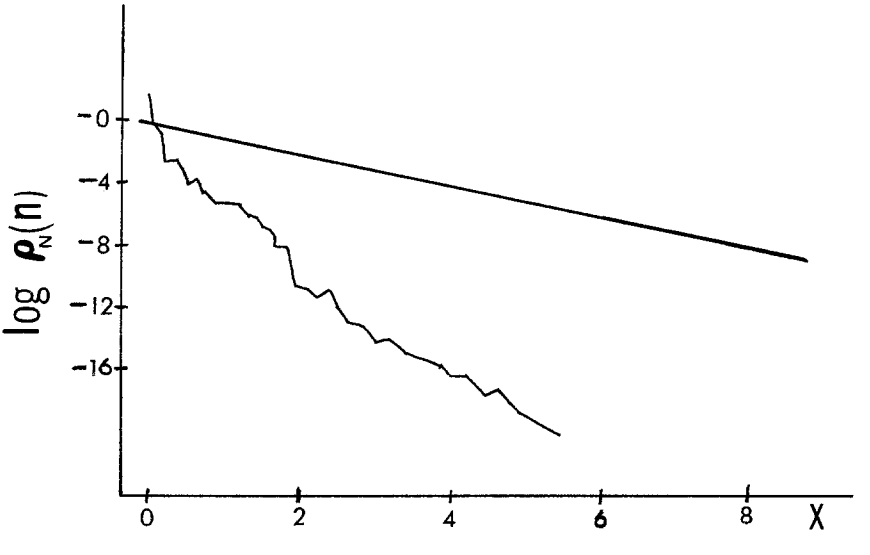

Fig. 2. A plot of the same variables as in Fig. 1 but for $k = 10$ and $\tau = 1/2$. Here the curves are quite distinct indicating a lack of stochasticity in the quantum motion even though $K = 5$ as in Fig. 1. We do not yet understand this quantum anomaly.

quantum anomalies which we shall discuss in the next section.

In order to summarize all the computed data for the above two runs plus two additional ones, we list the various computed parameters in Tables I-IV which appear at the end of this section. In each table, the first column lists the value of the integer time t. The second column lists the normalized average energy $\langle E \rangle_N$ at each time normalized in such a way that were the system motion stochastic exhibiting the Gaussian distribution (30) then the table values for $\langle E \rangle_N$ would sequentially read 1, 2, 3, 4, and 5; in particular $\langle E \rangle_N$ is given by

$$\langle E \rangle_N = \langle E \rangle / (k^2 t_1 / 4) \ , \tag{31}$$

where t_1 is the number of iterations per output. The third column lists a parameter B determined by a least squares fit of the experimental data to the formula

$$\rho_N(n) = A \ e^{-BX} \ . \tag{32}$$

If the motion were purely stochastic, B would equal unity. The fourth column lists a parameter W_d given by

$$W_d = [A/k(\pi t)^{1/2}] \int_{-\infty}^{\infty} \exp(-Bn^2/k^2 t) \ dn = A/B^{1/2} \ ; \tag{33}$$

loosely speaking, W_d is related to the percentage of stochastic energy diffusion in the motion. For purely stochastic motion, we would find $W_d = 1$. The fifth column lists (W_d/B) which is the average energy computed using the fitted Eq. (32) and given by

$$\langle E \rangle = A \int_{-\infty}^{\infty} (n^2/2) \ e^{-BX} \ dn = W_d/B \ . \tag{34}$$

The sixth column lists the ratio ξ given by

$$\xi = \langle E \rangle \ / \ \langle E \rangle_d \ , \tag{35}$$

TABLE I. A listing of stochastic energy absorbtion parameters as a function of time for one computer solution of the driven quantum pendulum. The parameters are defined in the text. Here k = 40, τ = 1/8, and K = kτ = 5. The number of $b_s(k)$ values used in Eq. (24) was 101.

t	$\langle E \rangle_N$	B	W_d	W_d/B	ξ	R_o	$\lvert a_o \rvert^2$
5	1.55	3.67	331	90.3	1.55	0.38	0.0024
10	2.79	2.49	92.6	37.3	1.39	1.36	0.0061
15	3.77	0.76	0.90	1.18	1.26	1.01	0.0037
20	5.01	0.75	0.87	1.16	1.25	1.67	0.0053
25	5.66	0.83	0.87	1.05	1.13	1.43	0.0040

TABLE II. A listing of stochastic energy absorbtion parameters as a function of time for one computer solution of the driven quantum pendulum. Here k = 40, τ = 1/40, and K = kτ = 1. The number of N of $b_s(k)$ values used in Eq. (24) was 101.

t	$\langle E \rangle_N$	B	W_d	W_d/B	ξ	R_o	$\lvert a_o \rvert^2$
30	0.089	29.1	0.28	0.0096	0.0056	16.50	0.043
60	0.100	53.2	0.27	0.0051	0.0029	6.70	0.012
90	0.068	76.4	0.24	0.0031	0.0018	9.48	0.014
120	0.077	94.2	0.14	0.0015	-0.0005	4.89	0.0063
150	0.048	116.0	0.15	0.0013	-0.0002	25.4	0.028

where $\langle E \rangle$ is given by Eq. (27) and

$$\langle E \rangle_d = (k^2/4)t \tag{36}$$

is essentially Eq. (10) expressed in terms of the quantum parameters or, alternatively, it is $\langle n^2/2 \rangle$ computed using Eq. (29). If the motion were completely stochastic, the fifth and sixth columns of each table would be identical. The seventh column lists the ratio $R_o = |A_o|^2 k(\pi t)^{1/2}$ of the actual probability of the zeroth energy level to that expected from the Gaussian distribution of Eq. (29). The last column lists

$|A_o|^2$ itself. The number of Bessel functions (or $b_s(k)$) needed in Eq. (22) to accurately compute each run is listed in the table captions. Finally, in all four runs at least 1,000 A_n-values ($-500 \lesssim n \lesssim 500$) were computed at each iteration and, as mentioned earlier, accuracy was checked by verifying normalization of the A_n-sum.

We now turn to a discussion of these experimental results.

V. DISCUSSION OF NUMERICAL RESULTS

We have presented results for four runs selected to illustrate typical behavior in a modest variety of k and τ ranges. The parameter values $k = 40 >> 1$ and $\tau = 1/8 << 1$ (corresponding to a classical $K = 5$) used in the computations yielding Fig. 1 and Table I are those for which one would expect quantum stochastic behavior, since the corresponding classical system is certainly highly stochastic for this case. A survey of Fig. 1 and Table I reveal that these expectations are verified reasonably well. However, it must be emphasized that our calculations yield a solution only over a finite time interval, that the computed $\rho(n)$ distribution contains large fluctuations, and that the various parameters in Table I are only crude indices which do deviate from their expected values. Pending further study, our results here must be regarded as providing only an indication of

TABLE III. A listing of stochastic energy absorbtion parameters as a function of time for one computer solution of the driven quantum pendulum. Here $k = 1$, $\tau = 5$, $K = k\tau = 5$. The number N of $b_s(k)$ values used in Eq. (24) was 23.

t	$\langle E \rangle_N$	B	W_d	W_d/B	ξ	R_o	$\lvert a_o \rvert^2$
150	0.0108	13.1	0.023	1.78×10^{-3}	3.18×10^{-4}	12.6	0.58
300	0.0092	29.5	0.029	9.83×10^{-4}	-7.50×10^{-6}	27.9	0.91
450	0.0079	40.0	0.015	3.70×10^{-4}	-4.60×10^{-5}	22.9	0.61
600	0.0057	55.4	0.015	2.80×10^{-4}	-2.50×10^{-5}	38.2	0.88
750	0.0079	66.2	0.020	2.96×10^{-4}	1.90×10^{-6}	35.9	0.74

TABLE IV. A listing of stochastic energy absorbtion parameters as a function of time for one computer solution of the driven quantum pendulum. Here k = 10, τ = 1/2, and K = kτ = 5. The number of N of $b_s(k)$ values used in Eq. (24) was 41.

t	$\langle E \rangle_N$	B	W_d	W_d/B	ξ	R_o	$\lvert a_o \rvert^2$
90	0.27	1.12	0.055	0.049	0.27	1.24	0.073
180	0.27	1.71	0.066	0.039	0.13	4.44	0.019
270	0.32	2.43	0.077	0.032	0.10	4.55	0.016
360	0.26	2.93	0.066	0.023	0.066	4.74	0.014
450	0.30	3.75	0.070	0.024	0.061	4.86	0.013

quantum stochastic behavior for the above parameter values.

The parameter values k = 40 and τ = 1/40 (classical K = 1) used for Table II are those which classically lie on the border of stochasticity, and the data presented in Table II clearly indicates that the quantum behavior for this case is also non-stochastic. Table III which presents results for k = 1 and τ = 5 (classical K = 5) indicates that the quantum motion is non-stochastic even though the corresponding classical motion is stochastic. However, as mentioned earlier, this difference between the quantum and classical case is understandable and to be expected. For small k values, the impulses or "kicks" do not give rise to many $e^{in\theta}$ "harmonics" in Eq. (22), and thus energy cannot be absorbed into many energy levels as is the case for k>>1 where 2k "harmonics" are involved. This dependence of quantum stochasticity on k and not just the product (kτ) as in the classical case receives support from the calculations resulting in Table III, but more work will be required to establish the approximate k-value determining the border of quantum stochasticity.

The results presented in Table IV and Fig. 2 which involve k = 10 and τ = 1/2 constitute a true puzzle, since here k>>1 and the corresponding classical K = 5 just as for Table I and Fig. 1. Thus one might have expected stochastic behavior rather than the stable, non-stochastic data which actually appears. It is possible that the stochastic border occurs for higher k-values than previously anticipated, or it is possible that one here is observing a totally new and unexpected

effect; only further study can reveal the appropriate and correct alternative. In this regard, let us mention that there are further unique quantum effects. For example regardless of k-value or initial $\psi(\theta,0)$, the free rotation mapping of Eq. (15) is the identity map when $\tau = 4\pi$; for this τ-value after an integer number t of "kicks", we have from Eq. (19) that

$$\psi(t) = \psi(0) \exp[itk\cos\theta] \tag{37}$$

which yields the average energy growth given by

$$\langle E\rangle = -(\hbar^2/2m\ell^2) \int d\theta\psi^*(\partial^2/\partial\theta^2)\psi \sim t^2 \tag{38}$$

that is proportional to t^2, corresponding to resonant rather than diffusive energy absorption. Moreover, when $\tau = 2\pi$, one may use Eq. (24) and a well-known Bessel function identity[11] to rigorously prove that $A_n(t+2T^+) = A_n(t)$ for all n; that is, the full driven quantum solution is strictly periodic independent of $\psi(\theta,0)$ or the value of k. Finally, resonant energy growth proportional to t^2 has also been observed for $\tau = 4\pi/m$, where m = 3, 4, 8, and 32, although the τ-widths of these resonances become increasingly narrow as m increases. Apparently, these peculiar resonant (or anti-resonant at $\tau = 2\pi$) effects are due to the strictly periodic nature of the unperturbed free rotator wave function; while all unperturbed classical rotator orbits are periodic, there is no period common to all solutions as occurs in the quantum case.

Subsequent to the Como Conference, we continued the above Fig. 1-run for k = 40 and $\tau = 1/8$ and discovered that the diffusive quantum energy absorption obeys Eq. (29) up to a time t_B (break-time) after which diffusive energy absorption appears to continue but at a much slower rate. Empirically, we find t_B proportional to k in sequences of runs for which $K = (k\tau)$ is held fixed. This result further "explains" the lack of any diffusive energy absorption in the data of Table III where k = 1 and $\tau = 5$ which is classically stochastic. A very crude, but possible explanation for the appearance of this break-time t_B may lie in the uncertainty relationship $\Delta E\Delta t \sim \hbar$. Note in Eq. (17) and Eq. (18) that the classical limit $\hbar \to 0$ is equivalent to $k \to \infty$ and $\tau \to 0$. Thus for large k and small τ ($\hbar$ fixed), we might expect the quantum behavior to mimic the classical at least for a time interval Δt during which the discrete nature of the free rotator energy level spectrum is insignificant. From Eq. (15), one

notes that τ is a measure of the "effective" energy level spacing. Thus taking $\Delta E \sim \tau$ and $\Delta t \sim t_B$ in $\Delta E \Delta t \sim \hbar$, we have $t_B \sim \tau^{-1} \sim k$ for fixed $K(=k\tau)$, where t_B is the time required for the quantum system to "notice" that its energy levels are discrete. Further numerical study will be required to verify this possible explanation.

In closing this section, let us mention that we have sought to verify a sensitive dependence of final quantum state upon initial state similar to that implied by the exponential separation[3] of initially close classical orbits. Holding $K = k\tau$ fixed, we have tried k-values from k = 1 to k = 100 using various pairs of initially close $\{A_n(0)\}$ initial states only to find that the final state probability distribution $\rho(n) = A_n^* A_n$ was identical for each member of a pair to within numerical error. Even starting from non-close initial states such as $A_n = A_o \delta_{no}$ and $A_n = e^{-n^2}$ yielded the same final $A_n^* A_n$ distribution. Each of these initial quantum states (for large k and small τ) appeared to be approaching the unique final state probability distribution given by Eq. (29), at least for times $t < t_B$. Moreover, Eq. (29) is being approached from each of these definite initial states without the need for a time or an ensemble average. These rather startling results tempt one to speculate that the unique final state probability distribution for an isolated (chaotic) quantum system might be the microcanonical distribution, however premature such a speculation might be. Regardless of such speculations however, our present computations reveal no sensitive dependence of final state upon initial state, indeed they indicate a surprising lack of such dependence. Certainly in the classical limit of sufficiently large k and sufficiently small $\tau (K = k\tau >> 1)$, initially close wave packets must exponentially separate, but apparently even k = 100 and $\tau = 0.05$ does not lie in the classical parameter range.

VI. CONCLUDING REMARKS

This progress report has been presented in order to expose an example of a whole category of classically chaotic Hamiltonian systems whose exact quantum behavior can be investigated, at least numerically. It is our belief that future studies of the type Hamiltonian models revealed here can provide substantial information regarding the nature of chaotic behavior in deterministic quantum systems. Certainly the calculations for the specific pendulum Hamiltonian system considered herein provide at least an initial indication of the surprises and the possibly significant results which may await future investigators.

Regardless of final outcome, it now appears that a new doorway to quantum chaos may have opened and this progress report is an invitation for others to join us in crossing over its threshold.

In closing, we wish to express our profound appreciation to Ya. G. Sinai, E. V. Shuryak, G. M. Prosperi, G. M. Zaslavsky, D. Shepelyansky, and F. Vivaldi for many enlightening discussions regarding these problems. During the period of final editing for this paper, we received a specially prepared, handwritten preprint describing some splendid related work from Michael Berry, N. L. Balazs, M. Tabor, and A. Voros concerning "kicked" free particle systems. We have enormous admiration for the willingness of these authors to share their independent discoveries with us prior to publication.

REFERENCES

1. V. I. Arnold and A. Avez, Ergodic Problems of Classical Mechanics (W. A. Benjamin, Inc., New York, 1968); J. Moser, Stable and Random Motions in Dynamical Systems (Princeton Univ. Press, Princeton, 1973); Z. Nitecki, Differentiable Dynamics (MIT Press, Cambridge, 1971).
2. G. M. Zaslavsky, Statistical Irreversibility in Nonlinear Systems (Nauka, Moskva, 1970, in Russian); J. Ford in Fundamental Problems in Statistical Mechanics, III, Edited by E. G. D. Cohen (North-Holland, Amsterdam, 1975).
3. B. V. Chirikov, "A Universal Instability of Many-Dimensional Oscillator Systems," Physics Reports (to appear 1979).
4. N. M. Pukhov and D. S. Chernasvsky, Teor. i. Matem. Fiz. 7, 219 (1971).
5. I. C. Percival, J. Phys. B6, 1229 (1973); J. Phys. A7, 794 (1974); N. Pomphrey, J. Phys. B7, 1909 (1974); I. C. Percival and N. Pomphrey, Molecular Phys. 31, 97 (1976).
6. K. S. J. Nordholm and S. A. Rice, J. Chem. Phys. 61, 203 (1974).
7. K. S. J. Nordholm and S. A. Rice, J. Chem. Phys. 61, 768 (1974).
8. E. V. Shuryak, Zh. Eksp. Teor. Fiz. 71, 2039 (1976).
9. G. M. Zaslavsky and N. N. Filonenko, Soviet Phys. JETP 38, 317 (1974). K. Hepp and E. H. Lieb in Lecture Notes in Physics, V. 38, Edited by J. Moser (Springer-Verlag, New York, 1974). A. Connes and E. Stormer, Acta Mathematica 134, 289 (1975).
10. John M. Greene, "A Method for Determining a Stochastic Transition," Preprint, Plasma Physics Laboratory, Princeton, New Jersey.

11. M. Abramowitz and I. A. Stegun, Handbook of Mathematical Functions (Dover Publications, Inc., New York, 1972), p. 363 and 385.